Hindawi Publishing Corporation
Journal of Nanomaterials
Volume 2007, Article ID 84745, 6 pages
doi:10.1155/2007/84745

Review Article

Rare Earth-Activated Silica-Based Nanocomposites

C. Armellini,[1] A. Chiappini,[1] A. Chiasera,[1] M. Ferrari,[1] Y. Jestin,[1] M. Mortier,[2] E. Moser,[3] R. Retoux,[4] and G. C. Righini[5,6]

[1] *CSMFO group, CNR-IFN, Istituto di Fotonica e Nanotecnologie, via Sommarive, 14-38050 Povo, Trento, Italy*
[2] *Laboratoire de Chimie Appliquéede de l'Etat Solide, Ecole Nationale Supérieure de Chimie de Paris (ENSCP), UMR-CNRS 7574, 11 rue Pierre et Marie Curie, 75231 Paris, France*
[3] *Dipartimento di Fisica, Università degli Studi di Trento, Gruppo CSMFO, Via Sommarive, 14-38100 Povo, Trento, Italy*
[4] *Laboratoire CRISMAT, UMR 6508, ENSICAEN, 6 Boulevard du Maréchal Juin, 14050 Caen Cedex, France*
[5] *CNR-IFAC, Istituto di Fisica Applicata, Nello Carrara, via Madonna del Piano, 10-50019 Sesto Fiorentino, Firenze, Italy*
[6] *CNR, Dipartimento Materiali e Dispositivi, via dei Taurini 19, 00185 Roma, Italy*

Received 3 August 2007; Accepted 23 November 2007

Recommended by Le Quoc Minh

Two different kinds of rare earth-activated glass-based nanocomposite photonic materials, which allow to tailor the spectroscopic properties of rare-earth ions: (i) Er^{3+}-activated SiO_2-HfO_2 waveguide glass ceramic, and (ii) core-shell-like structures of Er^{3+}-activated silica spheres obtained by a seed growth method, are presented.

1. INTRODUCTION

The recent developments of nanocomposite materials activated by rare-earth ions have opened new possibilities in the field of both basic and applied physics, in a large area covering information communication technologies, health and biology, structural engineering, and environment monitoring systems. As far as luminescence properties are concerned, Er^{3+}-activated nanocomposite glasses have become one of the key materials because of their relevance for to the development of optical amplifiers. The short-term goal is to develop appropriate material systems and devices to exploit, at the best, the luminescence properties of erbium with optimal optical properties of the host. The last decade has seen a remarkable increase in the experimental efforts to control and enhance emission properties of luminescent ions by tailoring the dielectric surrounding of the source [1–4]. With this aim, several approaches, using nanocomposite materials and/or specific geometries, such as planar interfaces, photonic crystals, solid state planar microcavities, dielectric nanospheres, and spherical microresonators, have been proposed.

The aim of this paper is to give an overview of the advances in glass-based photonic systems, where the nanoscale structures or the presence of nanostructured hosts induces an enhancement of optical and spectroscopic properties of the rare-earth ions. In particular, the following topics will be highlighted: (i) rare earth-activated glass-ceramics planar waveguides, where the active ions are embedded in the crystalline phase, combining the mechanical and optical properties of the glass with a crystal-like environment for the rare-earth ions, and (ii) a procedure for the synthesizing of monosize silica spheres and the fabrication of core-shell-like structures of Er^{3+}-activated silica spheres obtained by a seed growth method. Optical and spectroscopic assessment, as well as morphological and structural characterization of these systems, is reported.

2. TRANSPARENT GLASS-CERAMICS

Since the pioneer work in 1993, when Wang and Ohwaki discovered a novel glass-ceramic system characterized by a transparency comparable to glass [5], considerable efforts have been made in order to fabricate rare earth-activated glass-ceramic materials with active ions embedded in the crystalline phase [6]. The motivation for this research is combining the mechanical and optical properties of the glass with a crystal-like environment for the rare-earth ions, where their higher cross-sections can be exploited in order to fabricate more compact devices [4, 7]. Moreover, glass- ceramic materials may be a valid alternative method to control chemical parameters of the rare-earth ions, and thus may avoid undesirable effect like clustering as proposed by Auzel

and Goldner [8]. Thanks to the low phonon environment favourable to enhance the radiative rate and quantum efficiency, significant results have been achieved using oxyfluoride and fluoride transparent glass-ceramics activated by rare-earth ions, such as Er^{3+}, Eu^{3+}, Tm^{3+}, Nd^{3+}, and Pr^{3+} incorporated in fluoride nanocrystalline phases [9–14]. Using a top-down technique based on an appropriate thermal process of the glasses containing rare-earth fluorides, nanocrystals of β-PbF_2 were nucleated in the glassy matrix. Concerning telecom application, the paper by Hayashi et al. concerning Tm^{3+} ion-doped transparent oxyfluoride glass-ceramics containing PbF_2 nanocrystals around 20 nm in size, is of particular interest [15]. From spectroscopic measurements performed at low temperature, authors show the possibility of optical amplification in the S telecommunication band. Tikhomirov et al. have measured a bandwidth of about 90 nm for the $^4I_{13/2} \rightarrow {}^4I_{15/2}$ transition when Er^{3+}-activated oxyfluoride glass-ceramics were prepared with β-PbF_2 nanocrystals of about 2.5 nm in diameter [16].

Oxide-based glass-ceramics have been obtained both by conventional melting and by sol-gel route. Oishi et al. reported highly transparent glass ceramics obtained by heating, at 410–460°C, the K_2O-MgO-Nb_2 O_5-TeO_2 glass precursor activated by Er^{3+} and Eu^{3+} ions [17]. It was demonstrated that the addition of Er^{3+} and Eu^{3+} ions was effective for the formation of the crystalline phase showing second harmonic generation, as well as enhancing the NIR-to-green upconversion, in the case of Er^{3+}-activated glass ceramics [17]. Attractive results have been obtained by sol-gel route. Kępiński and Wołcyrz report on formation of nanocrystalline rare-earth silicates inside or at the surface of amorphous SiO_2 matrix upon heat treatment in air [18]. An intense room temperature photoluminescence at 1.531 μm is reported by Que et al. for erbium oxide nanocrystals dispersed in TiO_2/γ-glycidoxypropyltrimethoxysilane (GLYMO) composite sol-gel thin films [19].

It should be mentioned that these nanocomposite systems are of particular interest for photonic application when the glass-ceramics can be prepared in waveguiding configuration. Concerning this, Strohhöfer et al., ten years ago, reported on active optical properties of Er-containing crystallites in sol-gel derived glass films [20]. Authors employed controlled heat treatment procedures to obtain a certain fraction of the rare-earth ions in crystallites. The active phases precipitated were $Er_2Ti_2O_7$ and $ErPO_4$ in SiO_2-TiO_2-based sol-gel films. Doping of the glass matrix with Er^{3+}-containing crystallites improved the Er^{3+} fluorescence lifetime of the 1.55 μm transition, in some cases by more than 200%, unfortunately, no satisfactory waveguiding properties were achieved [20]. A pure $Er_2Ti_2O_7$ pyrochlore waveguiding structure was proposed by Langlet et al. with interesting spectroscopic properties because this compound has a much lower phonon energy than silica, which would permit to minimize nonradiative absorption mechanisms [21]. Recently, Jestin et al. have shown that SiO_2-HfO_2: Er^{3+} glass-ceramic planar waveguides prepared by sol-gel route present valuable optical, spectroscopic, and structural features for successful applications in the telecommunication area [22–24].

2.1. Glass-ceramics fabrication and characterization

(100-x)SiO_2-$x$$HfO_2$ (x = 10, 20, 30 mol) planar waveguides, activated by 0.3 mol % Er^{3+} ions, were prepared by sol-gel route, using dip-coating deposition on v-SiO_2 substrates cleaned by ultrasound and alcohol [24]. Depending on their HfO_2 molar content (x = 10, 20, 30 mol), the waveguides discussed in this section are labeled W10, W20, and W30, respectively. The starting solution obtained by mixing tetraethylorthosilicate (TEOS), ethanol, deionized water, and hydrochloric acid as a catalyst was prehydrolyzed for one hour at 65°C. The molar ratio of TEOS : HCl : EtOH : H_2O was 1 : 0.01 : 37.9 : 2. An ethanolic colloidal suspension was prepared using a precursor $HfOCl_2$, and then added to the TEOS solution with an Si/Hf molar ratio of 90/10, 80/20, and 70/30. Erbium was added as $Er(NO_3)_3 \cdot 5\,H_2O$ with an Er/(Si + Hf) molar concentration of 0.3 mol %. Erbium-activated silica-hafnia films were deposited on v-SiO_2 substrates by dip-coating with a dipping rate of 40 mm/min. Before further coating, each layer was annealed in air for 50 seconds at 900°C. Finally, the films, resulting of 30 coatings, were stabilized by a treatment in air and introduced directly in the furnace at 900°C (optimized temperature to fully densify the waveguides) for 5, 210 minutes, and 30 hours for the waveguides W30, W20, and W10, respectively. As a result of this procedure, transparent and crack-free waveguides were obtained. In order to nucleate nanocrystals inside the planar waveguide, an additional heat treatment was performed in air at a temperature of 1000°C for 30 minutes [22].

Specimens for high resolution transmission electron microscopy (HRTEM) observations were prepared by scraping off the thin films in ethanol using a diamond knife. A drop of the suspension is deposited and dried onto a carbon coated copper grid. A HRTEM study of the scraped samples was performed in a 200 kV side entry JEOL 2010 FEG by transmission electron microscope (TEM) fitted with a double-tilt sample holder (tilt ±30°).

The losses at 1542 nm, for the TE_0 mode, were evaluated using the moving fiber method in which the exponential decay of light is measured by a fiber probe scanning down the length of the propagating steak [25]. The TE_0 mode waveguiding excitation was used for photoluminescence (PL) measurements. PL measurements in the region of the $^4I_{13/2} \rightarrow {}^4I_{15/2}$ transitionand the decay curves from the $^4I_{13/2}$ level were obtained using the 514 nm line of a CW argon laser as an excitation source, and dispersing the luminescence light with a 320 mm single-grating monochromator with a resolution of 2 nm, with the experimental setup described elsewhere [22, 23, 26].

2.2. Glass-ceramics results and discussion

Nanostructured morphology of the sample W30, annealed at 1000°C for 30 minutes, was analyzed by means of HRTEM. The HRTEM images of a scrapped part of the film presented in Figures 1(a) and 1(b) show nanocrystals of about 4 nm to 6 nm in size, homogeneously dispersed in the amorphous matrix. Figure 1(b) evidences that each nanocrystal presents single domain features. The EDS analysis confirmed that

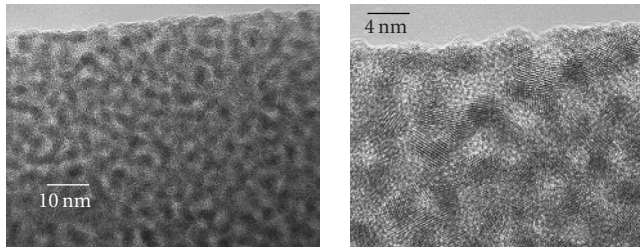

Figure 1: HRTEM image of the silica-hafnia W30 sample, annealed at 1000°C for 30 minutes, showing HfO_2 nanocrystals homogeneously dispersed in the amorphous matrix (a). Single domain nanocrystals are clearly evidenced in (b).

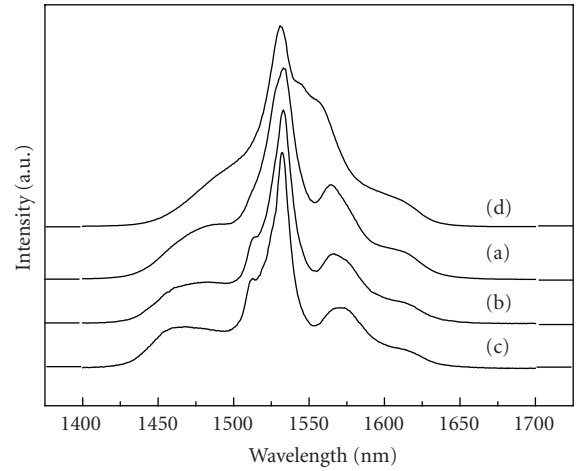

Figure 2: Room temperature luminescence spectra, obtained by exciting the TE_0 mode at 514.5 nm, of the $^4I_{13/2} \rightarrow {}^4I_{15/2}$ transition of Er^{3+} ion for the (a) W10, (b) W20, and (c) W30 planar waveguides annealed at 1000°C for 30 minutes. The emission spectrum of the W30 amorphous waveguide annealed at 900°C for 5 minutes is also reported for comparison (d).

the nanocrystals and the surrounding amorphous matrix are composed of Hf oxide and Si oxide, respectively.

The glass-ceramic waveguides present a thickness of 1.3, 1.15, and 1 μm, and a refractive index close to 1.485, 1.538, and 1.597 measured at 1532 nm in the TE polarization for W10, W20, and W30, respectively. They are all a single mode at 1.5 μm, and the refractive index is highly dependent on the hafnium concentration. The losses of about 1 dB cm^{-1} measured at 1542 nm, for this kind of glass-ceramics, make them suitable for operation in the C telecommunication band.

Figure 2 shows the normalized PL spectra for the glass-ceramic W10, W20, and W30 waveguides in the region of the $^4I_{13/2} \rightarrow {}^4I_{15/2}$ transition of Er^{3+} ions. The changes in the shape and bandwidth, with respect to the shape usually observed in the amorphous silica hafnia system (Figure 2(d)) [22, 26], indicate the significant modification of erbium ions environment in glass-ceramic systems. PL spectra show that Stark components are better resolved in the glass-ceramic, indicating that the Er^{3+} environment is more crystalline like. As the Er^{3+} local environment becomes ordered, it limits the inhomogeneous broadening typical of glassy environment, and therefore, the bandwidth narrows. The spectral width measured at 3 dB from the maximum intensity is 28, 19, 17 ± 1 nm for W10, W20, and W30 glass ceramic waveguides, respectively. Note that the bandwidth of the planar waveguide annealed at 900°C for 5 minutes, which is amorphous, is 51 ± 1 nm (see Figure 2(d)).

The decay curves of the luminescence from the $^4I_{13/2}$ metastable state of Er^{3+} ions exhibit a single exponential profile for W20 and W30 glass-ceramics, and a double exponential profile for W10 sample. This nonsingle exponential profile is explained by the fact that not all erbium ions are feeling the same local environment. By fitting the decay curves with two different single exponential profiles, we can notice two different contributions: one corresponding to the erbium ions in the glass matrix leading to a lifetime close to 7.0 milliseconds, and the second part corresponding to erbium ions embedded in the crystalline environment leading to a lifetime close to 9 milliseconds. In the case of W20 and W30, as the decay profiles are single exponential, we can assume that all erbium ions are embedded in the crystalline environment. The decrease of the lifetime of Er in crystals from 9 milliseconds to 8.7 and 7.2 milliseconds, as the HfO_2 content increases from 10% to 20% and to 30%, is attributed to an increase of the radiative electric dipole transition rate in a hafnia-dominated local field [24, 27]. The shortening of the lifetime with the increasing of HfO_2 content was already observed also for amorphous waveguides. Zampedri et al. have shown that in the case of $(100\text{-}x)SiO_2$-$xHfO_2$ waveguides(x = 10, 20, 30, 40 mol), the $^4I_{13/2}$ lifetime decreases from 7.1 milliseconds to 5.5 milliseconds when the HfO_2 content increases from 10 mol % to 40 mol % [28]. They invoke the role of hafnia in increasing both distortion and crystal field strength around the Er^{3+} ion. However, this effect surely deserves further experimental investigation. Besides, computer simulation could be useful to take into account possible differences in the chemical environment of Er^{3+} ion for waveguides of different composition.

3. CORE-SHELL-LIKE STRUCTURES BY SOL-GEL-DERIVED ER^{3+}-ACTIVATED SILICA NANOSPHERES

Monodisperse colloidal spheres in solution can be self-organized into an ordered structure if their size is adequate and their size polydispersivity is low enough, yielding a periodic photonic bandgap structure or photonic crystal [29]. Furthermore, monodisperse colloidal spheres of predictable size and shape, activated with a controllable concentration of rare-earth ions like Er^{3+}, have significant potential for use in optical devices such as microlasers, integrated optics structures, luminescent markers or nanosensors, and active photonic bandgap materials. In particular, in order to use rare-earth-activated colloids in photonic crystals, it is well known that the size polydispersivity of the particles needs to be low and controllable.

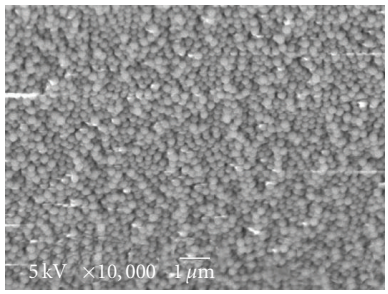

Figure 3: SEM images of the core-shell-like particles after seeded growth using the acid-based reaction.

3.1. Core-shell-like Er^{3+}-activated silica spheres fabrication and characterization

The core-shell-like Er^{3+}-activated silica spheres, where the core is the silica sphere and the shell is an Er_2O_3-SiO_2 coating, were prepared using the following protocol: (i) the core was realized using the Stober method, discussed in detail in [30]. and (ii) the shell was obtained by a seeded growth method [31]. Briefly, 150 mg of silica spheres of 270 nm diameter, obtained by the Stober method, were added to a solution with the molar ratio TEOS : CH_3COOH : H_2O of 1 : 8 : 8, plus 0.2 wt% of $ErCl_3$. The mixture was stirred for 45 minutes with a magnetic stirrer. After synthesis, the SiO_2 particles were separated from the solution by centrifuging at 1000 rpm and washed at least twice with pure ethanol. Subsequently, the core-shell-like Er^{3+}-activated silica spheres were heat treated at 950°C for 30 minutes [32].

The particle sizes were determined from electron micrographs taken with a scanning electron microscope, (SEM: JEOL-JSM 6300). The diameters of over a hundred particles were used in calculations of the average size and standard deviation δ of each sample. For photoluminescence spectroscopy on core-shell-like structures, the experimental setup described above for glass-ceramics was employed. The photoluminescence measurements were performed on pressed KBr pellets, containing 5% of doped silica spheres.

3.2. Core-shell-like Er^{3+}-activated silica spheres results and discussion

Figure 3 shows an SEM image of the core-shell-like Er^{3+}-activated silica spheres, obtained using a seeded growth method on the 270 nm monosize silica spheres. Figure 4 presents the PL spectra for the core-shell-like structure in the region of the $^4I_{13/2} \rightarrow {}^4I_{15/2}$ transition of Er^{3+} ions, obtained upon excitation at 980 nm.

The SEM image of Figure 3 demonstrates that seeded growth in the Er solution occurs on individual particles that do not collapse in higher-size clusters. PL measurements confirm the incorporation of Er^{3+} ions in the silica shell. In fact, the shape of the emission band in Figure 4 is typical of Er^{3+}-activated silica glasses with a main emission peak at 1533 nm [33] and a spectral bandwidth, measured at 3 dB from the maximum intensity of 27 ± 2 nm.

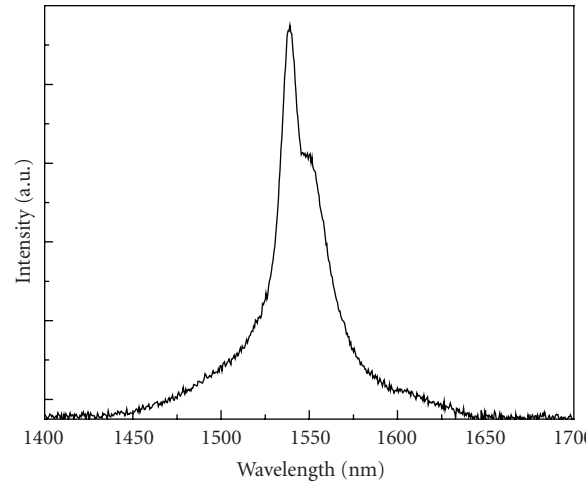

Figure 4: Room temperature photoluminescence spectra of $^4I_{13/2} \rightarrow {}^4I_{15/2}$ transition of the Er^{3+} ions for the silica core-shell-like structure upon excitation at 980 nm.

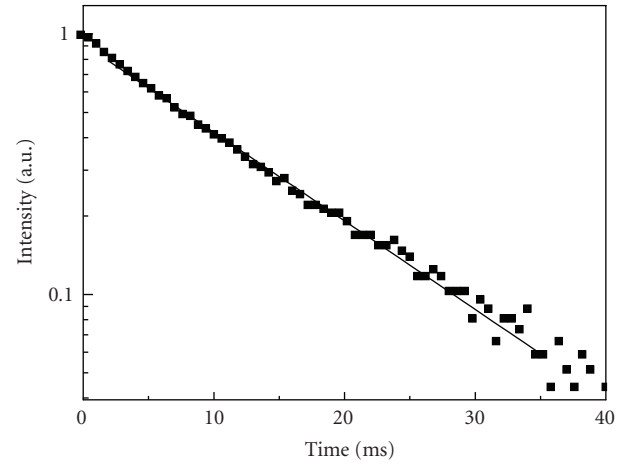

Figure 5: Room temperature luminescence decay curve from the $^4I_{13/2}$ state of Er^{3+} ions for the silica core-shell-like structure, upon excitation at 514.5 nm, after annealing for 30 minutes at 950°C.

The luminescence decay curve from the $^4I_{13/2}$ state of Er^{3+} ions for the silica core-shell-like structure, upon excitation at 514.5 nm, is reported in Figure 5. The decay profile exhibits a single exponential behavior with a lifetime of 12.8 ± 0.1 milliseconds. In order to give an estimation of the quantum efficiency η, defined by the ratio $\eta = \tau_{meas}/\tau_{rad}$, the measured lifetime (τ_{meas}) must be compared with the radiative lifetime τ_{rad}. Recently, many investigations were performed on SiO_2 spherical colloids doped with Er^{3+} ions in order to study the spontaneous emission and determine the local optical density of states in these systems [34, 35]. In these papers, Dood et al. determined a radiative lifetime of 18 ± 3 milliseconds for the $^4I_{13/2}$ state of Er^{3+} ions in pure silica. Note that this value is larger than the radiative lifetime reported for the $^4I_{13/2}$ state of Er^{3+} ions in silicate glasses [33]. Assuming a τ_{rad} of 18 milliseconds, a quantum efficiency η of 71% can be estimated for our core-shell spheres.

4. CONCLUSIONS

The paper presents some recent results in specific dielectric-based nanostructured and nanocomposite systems useful for the enhancement of Er^{3+} spectroscopic properties.

SiO_2-HfO_2: Er^{3+} glass-ceramic planar waveguides were prepared by sol-gel route, with nanocrystals of about 4 nm to 6 nm in size, homogeneously dispersed in the amorphous matrix. These waveguides exhibit a single mode at 1.5 μm, their refractive index is highly dependent on the hafnium concentration, and the attenuation coefficient is about 1 dB cm^{-1} at 1542 nm. The spectroscopic properties of Er^{3+} ions are determined by the crystalline local environment.

Seeded growth was successfully applied to synthesize core-shell-like Er^{3+}-activated silica spheres. Typical photoluminescence spectrum of erbium, with a lifetime of 12.8 milliseconds, was observed for the core-shell-like structure after annealing for 30 minutes at 950°C leading to a quantum efficiency of 71%.

ACKNOWLEDGMENTS

This research was partially supported by PAT (2004–2006) FAPVU and PAT (2007–2010) FaStFAL research projects. Part of this work has also been performed in the frame of the European forum on new glass applications (EFONGA) FP6 coordination action.

REFERENCES

[1] P. Moriarty, "Nanostructured materials," *Reports on Progress in Physics*, vol. 64, pp. 297–381, 2001.

[2] R. S. Meltzer, W. M. Yen, H. Zheng, et al., "Effect of the matrix on the radiative lifetimes of rare earth doped nanoparticles embedded in matrices," *Journal of Luminescence*, vol. 94-95, pp. 217–220, 2001.

[3] R. S. Meltzer, S. P. Feofilov, B. Tissue, and H. B. Yuan, "Dependence of fluorescence lifetimes of Y_2O_3:Eu^{3+} nanoparticles on the surrounding medium," *Physical Review B*, vol. 60, no. 20, pp. R14012–R14015, 1999.

[4] M. Mortier and F. Auzel, "Rare-earth doped transparent glass-ceramics with high cross-sections," *Journal of Non-Crystalline Solids*, vol. 256-257, pp. 361–365, 1999.

[5] Y. Wang and J. Ohwaki, "New transparent vitroceramics codoped with Er^{3+} and Yb^{3+} for efficient frequency upconversion," *Applied Physics Letters*, vol. 63, no. 24, pp. 3268–3270, 1993.

[6] M. C. Gonçalves, L. F. Santos, and R. M. Almeida, "Rare-earth-doped transparent glass ceramics," *Comptes Rendus Chimie*, vol. 5, no. 12, pp. 845–854, 2002.

[7] M. Mortier, "Between glass and crystal: glass-ceramics, a new way for optical materials," *Philosophical Magazine B*, vol. 82, no. 6, pp. 745–753, 2002.

[8] F. Auzel and P. Goldner, "Towards rare-earth clustering control in doped glasses," *Optical Materials*, vol. 16, no. 1-2, pp. 93–103, 2001.

[9] V. K. Tikhomirov, V. D. Rodríguez, J. Méndez-Ramos, P. Núñez, and A. B. Seddon, "Comparative spectroscopy of (ErF_3)(PbF_2) alloys and Er^{3+}-doped oxyfluoride glass-ceramics," *Optical Materials*, vol. 27, no. 3, pp. 543–547, 2004.

[10] L. L. Kukkonen, I. M. Reaney, D. Furniss, M. G. Pellatt, and A. B. Seddon, "Nucleation and crystallisation of transparent, erbium III-doped, oxyfluoride glass-ceramics," *Journal of Non-Crystalline Solids*, vol. 290, no. 1, pp. 25–31, 2001.

[11] M. Mattarelli, V. K. Tikhomirov, A. B. Seddon, et al., "Tm^{3+}-activated transparent oxy-fluoride glass-ceramics: structural and spectroscopic properties," *Journal of Non-Crystalline Solids*, vol. 345-346, pp. 354–358, 2004.

[12] F. Liu, Y. Wang, D. Chen, and Y. Yu, "Investigation on crystallization kinetics and microstructure of novel transparent glass ceramics containing Nd:$NaYF_4$ nano-crystals," *Materials Science and Engineering B*, vol. 136, no. 2-3, pp. 106–110, 2007.

[13] G. Dantelle, M. Mortier, D. Vivien, and G. Patriarche, "Influence of Ce^{3+} doping on the structure and luminescence of Er^{3+}-doped transparent glass-ceramics," *Optical Materials*, vol. 28, no. 6-7, pp. 638–642, 2006.

[14] M. Mortier, A. Bensalah, G. Dantelle, G. Patriarche, and D. Vivien, "Rare-earth doped oxyfluoride glass-ceramics and fluoride ceramics: synthesis and optical properties," *Optical Materials*, vol. 29, no. 10, pp. 1263–1270, 2007.

[15] H. Hayashi, S. Tanabe, and T. Hanada, "1.4 μm band emission properties of Tm^{3+} ions in transparent glass-ceramics containing PbF_2 nanocrystals for S-band amplifier," *Journal of Applied Physics*, vol. 89, no. 2, pp. 1041–1045, 2001.

[16] V. K. Tikhomirov, D. Furniss, A. B. Seddon, et al., "Fabrication and characterization of nanoscale, Er^{3+}-doped, ultratransparent oxyfluoride glass-ceramics," *Applied Physics Letters*, vol. 81, no. 11, pp. 1937–1939, 2002.

[17] H. Oishi, Y. Benino, and T. Komatsu, "Preparation and optical properties of transparent tellurite based glass-ceramics doped by Er^{3+} and Eu^{3+}," *Physics and Chemistry of Glasses*, vol. 40, no. 4, pp. 212–218, 1999.

[18] L. Kępiński and M. Wołcyrz, "Nanocrystalline rare earth silicates: structure and properties," *Materials Chemistry and Physics*, vol. 81, no. 2-3, pp. 396–400, 2003.

[19] Q. Que, Y. Zhou, Y. L. Lam, et al., "Photoluminescence of erbium oxide nanocrystals/Tio_2/γ-glycidoxypropyltrimethoxysilane (GLYMO) composite sol-gel thin films derived at low temperature," *Journal of Applied Physics*, vol. 89, no. 5, pp. 3058–3060, 2001.

[20] C. Strohhöfer, J. Fick, H. C. Vasconcelos, and R. M. Almeida, "Active optical properties of Er-containing crystallites in sol-gel derived glass films," *Journal of Non-Crystalline Solids*, vol. 226, no. 1-2, pp. 182–191, 1998.

[21] M. Langlet, C. Coutier, J. Fick, et al., "Sol-gel thin film deposition and characterization of a new optically active compound: $Er_2Ti_2O_7$," *Optical Materials*, vol. 16, no. 4, pp. 463–473, 2001.

[22] Y. Jestin, N. Afify, C. Armellini, et al., "Er^{3+} activated silica-hafnia glass-ceramics planar waveguides," in *Integrated Optics, Silicon Photonics, and Photonic Integrated Circuits*, vol. 6183 of *Proceedings of SPIE*, pp. 1–8, Strasbourg, France, April 2006.

[23] Y. Jestin, C. Arfuso-Duverger, C. Armellini, et al., "Ceramization of erbium activated planar waveguides by bottom up technique," in *Optical Components and Materials IV*, vol. 6469 of *Proceedings of SPIE*, pp. 1–9, San Jose, Calif, USA, January 2007.

[24] Y. Jestin, C. Armellini, A. Chiappini, et al., "Erbium activated HfO_2 based glass-ceramics waveguides for photonics," *Journal of Non-Crystalline Solids*, vol. 353, no. 5–7, pp. 494–497, 2007.

[25] Y. Okamura, S. Yoshinaka, and S. Yamamoto, "Measuring mode propagation losses of integrated optical waveguides: a simple method," *Applied Optics*, vol. 22, no. 23, pp. 3892–3894, 1983.

[26] R. R. Gonçalves, G. Carturan, L. Zampedri, et al., "Sol-gel erbium-doped silica-hafnia planar and channel waveguides," in *Rare-Earth-Doped Materials and Devices VII*, vol. 4990 of *Proceedings of SPIE*, pp. 111–120, San Jose, Calif, USA, January 2003.

[27] N. D. Afify, G. Dalba, C. Armellini, M. Ferrari, F. Rocca, and A. Kuzmin, "Local structure around Er^{3+} in SiO_2-HfO_2 glassy waveguides using EXAFS," *Physical Review B*, vol. 76, Article ID 024114, 8 pages, 2007.

[28] L. Zampedri, G. C. Righini, H. Portales, et al., "Sol-gel-derived Er-activated SiO_2-HfO_2 planar waveguides for 1.5 μm application," *Journal of Non-Crystalline Solids*, vol. 345-346, pp. 580–584, 2004.

[29] A. Chiappini, C. Armellini, S. N. B. Bhaktha, et al., "Fabrication and optical assessment of sol-gel-derived photonic bandgap dielectric structures," in *Photonic Crystal Materials and Devices III*, vol. 6182 of *Proceedings of SPIE*, pp. 1–10, Strasbourg, France, April 2006.

[30] A. Chiappini, C. Armellini, A. Chiasera, et al., "Design of photonic structures by sol-gel-derived silica nanospheres," *Journal of Non-Crystalline Solids*, vol. 353, no. 5–7, pp. 674–678, 2007.

[31] G. H. Bogush, M. A. Tracy, and C. F. Zukoski IV, "Preparation of monodisperse silica particles: control of size and mass fraction," *Journal of Non-Crystalline Solids*, vol. 104, no. 1, pp. 95–106, 1988.

[32] M. J. A. de Dood, B. Berkhout, C. M. van Kats, A. Polman, and A. van Blaaderen, "Acid-based synthesis of monodisperse rare-earth-doped colloidal SiO_2 spheres," *Chemistry of Materials*, vol. 14, no. 7, pp. 2849–2853, 2002.

[33] W. J. Miniscalco, "Erbium-doped glasses for fiber amplifiers at 1500 nm," *Journal of Lightwave Technology*, vol. 9, no. 2, pp. 234–250, 1991.

[34] M. J. A. de Dood, L. H. Slooff, A. Polman, A. Moroz, and A. van Blaaderen, "Modified spontaneous emission in erbium-doped SiO_2 spherical colloids," *Applied Physics Letters*, vol. 79, no. 22, pp. 3585–3587, 2001.

[35] M. J. A. de Dood, L. H. Slooff, A. Polman, A. Moroz, and A. van Blaaderen, "Local optical density of states in SiO_2 spherical microcavities: theory and experiment," *Physical Review A*, vol. 64, no. 3, Article ID 033807, 7 pages, 2001.